SCIENTIFIC REPORTS
nature research

Check for updates

OPEN

Spatiotemporal distribution of ground-level ozone in China at a city level

Guangfei Yang ✉, Yuhong Liu & Xianneng Li

In recent years, ozone (O_3) pollution in China has shown a worsening trend. Due to the vast territory of China, O_3 pollution is a widespread and complex problem. It is vital to understand the current spatiotemporal distribution of O_3 pollution in China. In this study, we collected hourly data on O_3 concentrations in 338 cities from January 1, 2016, to February 28, 2019, to analyze O_3 pollution in China from a spatiotemporal perspective. The spatial analysis showed that the O_3 concentrations exceeded the limit in seven geographical regions of China to some extent, with more serious pollution in North, East, and Central China. The O_3 concentrations in the eastern areas were usually higher than those in the western areas. The temporal analysis showed seasonal variations in O_3 concentration, with the highest O_3 concentration in the summer and the lowest in the winter. The weekend effect, which occurs in other countries (such as the USA), was found only in some cities in China. We also found that the highest O_3 concentration usually occurred in the afternoon and the lowest was in the early morning. The comprehensive analysis in this paper could improve our understanding of the severity of O_3 pollution in China.

Air pollution has rapidly increased over the last few decades due to urbanization and industrialization, and this increase has attracted attention around the world, including in China. In 2012, the National Ambient Air Quality Standards (NAAQS) (GB 3095-2012) was published by the Chinese Ministry of Environmental Protection, which identified six environmental pollutants: sulfur dioxide (SO_2), nitrogen dioxide (NO_2), carbon monoxide (CO), ozone ($O_{3)}$, and particulate matter ($PM_{2.5}$ and PM_{10})[1–3]. Several air pollution control policies and programs have been established by the Chinese government[4–6]. However, there is still a gap between China's ambient air quality and the air quality guidelines (AQG) of the World Health Organization (WHO)[7]. In recent years, although the concentrations of most pollutants, including NO_2, SO_2, particulate matter, and CO, decreased in the period of 2013–2016, O_3 concentrations have increased by 10.79%[8]. O_3 has become a secondary pollutant after $PM_{2.5}$, which introduces new challenges to pollution control[9].

In the past few years, many studies have investigated the impact, formation, and sources of O_3 pollution. For instance, Khaniabadi *et al.*[10] found that inhaling high concentrations of O_3 or exposure to O_3-polluted environments for a long period of time had a negative impact on health. Inhaling high concentrations of O_3 can increase the risk of cardiovascular and respiratory diseases, which contribute to the overall mortality rate. Huang *et al.*[11] found that ambient O_3 exposure was related to the tremendous disease burden of chronic obstructive pulmonary disease in Ningbo, China, and the elderly comprised a more susceptible population. Existing evidence also reveals the adverse effects of O_3 on mental health[12]. O_3 pollution will not only have a negative impact on human health[13] but also have a variety of adverse effects on plants, such as declines in crop yields and quality[14–16]. Because O_3 has a negative impact on the transfer of nitrogen to grain, O_3 pollution will reduce the fertilizer efficiency of wheat[17], leading to the inhibition of net photosynthesis of wheat[18]. Additionally, O_3 is a secondary pollutant that is formed by other pollutants through reactions[19–21]. Therefore, the formation of O_3 pollution is affected by many factors[22–24]. Studies have shown that volatile organic compounds (VOCs) and NO_x are key precursors of O_3 formation[23]. Aromatic hydrocarbons and olefins are considered the main contributors to O_3 formation in many cities or regions in China. Ethylene, trans-pentene, propene, and BTEX (benzene, ethylbenzene, toluene, m-, p-, and o-xylene), as well as warm weather and low wind speeds, are also major contributors to O_3 formation[25]. Given that China is currently plagued by complex O_3 pollution problems, understanding the spatiotemporal pattern of O_3 pollution in China is of great significance for conducting environmental epidemiological studies and drafting appropriate regional O_3 pollution control strategies.

Institute of Systems Engineering, Dalian University of Technology, Dalian, China. ✉e-mail: gfyang@dlut.edu.cn

NAAQS		Who		
Grade 1	Grade 2	Air Quality Guidelines (AQG)	Interim target 1	High level
100	160	100	160	240

Table 1. The O_3 concentration limits of the NAAQS in China and the WHO (unit: $\mu g/m^3$).

Some scholars have launched investigations on the spatiotemporal pattern of O_3. In Nanjing, a unimodal peak was observed with the highest O_3 levels occurring from 14:00 to 15:00, and the O_3 concentration reached its maximum and minimum levels in the summer and winter, respectively[3]. Wang *et al.*[26] studied the ground-level O_3 concentrations of 6 major Chinese cities located on both sides of the Heihe-Tengchong line, and they found that ground-level O_3 concentrations exhibited monthly variability, peaking in summer and reaching the lowest levels in winter. The diurnal cycle reached a minimum in the morning and peaked in the afternoon. Some research has found that the O_3 distribution pattern is also related to terrain features[9,27].

As previously mentioned, most of the studies on O_3 spatiotemporal patterns are carried out with a short time scale and low spatial resolution and generally focus on a specific city or a limited spatial region. To the best of our knowledge, there has been a lack of research on the spatiotemporal pattern of O_3 in China using a higher spatial resolution and long time-series datasets. Recently, China established a large-scale ground real-time air quality monitoring network, which provides data we can use to conduct research on the spatiotemporal distribution pattern of O_3 pollution nationwide.

In brief, this research makes the following contributions. First, we obtained the O_3 concentration data of 338 cities across China for more than three years, covering 1-Jan-2016 to 28-Feb-2019. In terms of spatial perspective, we investigated the O_3 concentrations in seven major geographic regions and three major urban agglomerations to conduct a more in-depth analysis and discussion. In terms of temporal perspective, we studied the annual, seasonal, monthly, weekly, daily, and diurnal and nocturnal variations in the O_3 concentrations. Second, the reasons for different patterns in different regions were briefly analyzed. The research results from this large dataset can not only help us elaborate on the spatiotemporal distribution pattern of O_3 concentration in China with a better spatiotemporal resolution and increase public awareness of the current O_3 pollution situation in China but also assist the relevant departments in formulating more targeted O_3 pollution prevention and control policies to meet the NAAQS and even the AQG standards in the future.

Results and Discussion

The NAAQS and the WHO set concentration limits for the maximum daily 8-hour average (MDA8) O_3 concentration. Two levels of limits are specified in the NAAQS (Grade 1 and Grade 2), and three levels of limits are specified in the WHO standard (AQG, Interim target 1 and High level) (see Table 1).

Spatial distribution of O_3 in China. Figure 1 shows the spatial distributions of the O_3 concentrations in 338 cities in China in 2016–2018. The regions with the most O_3 pollution were mainly concentrated in North China and Central China, especially in the Beijing-Tianjin-Hebei region (BTH) region. In addition, the O_3 pollution in the Chengdu-Chongqing and the Pearl River Delta region (PRD) regions was significantly higher than that of their neighboring regions. O_3 pollution in China has shown a trend of outward expansion. As shown in Table 2, based on the statistical results of the 90th percentile of the maximum daily 8-hour average urban O_3 concentration, the top 10 cities with severe O_3 pollution are mainly located in North China, Central China and the East China.

Fig. 2 displays the over-standard rate of the O_3 concentration in seven geographical regions in China. None of the cities in North China met the AQG or Grade 1 limit, and nearly 70% exceeded the Grade 2 limit. In East and Central China, nearly 40% of urban O_3 concentrations exceeded the Grade 2 limit. The O_3 pollution in other regions was not so prominent; however, there were still considerable gaps from the AQG standard.

O_3 is a secondary pollutant, which is generally formed in the atmosphere through photochemical pathways of NOx and volatile organic compounds (VOCs)[28–32]. Most of the NO_x and VOCs come from heavy industries, such as coal-fired power plants, the steel industry, and the cement industry. Some studies found that the local photochemical reaction process has made an important contribution to the formation of O_3[33], including the consumption of NO_2 during the photochemical reaction process[23], which has been observed in regions such as North China and Yangtze River Delta (YRD) region[34,35].

Additionally, PM pollution control in these regions has achieved certain results, and the reduction in haze has led to increased visibility, which in turn, has promoted the process of photochemical reactions and promoted the formation of O_3 pollution. It is worth noting that some cities in western China, where industrial activities are infrequent, sometimes have high concentrations of O_3. In these high-altitude regions, the increase in O_3 concentration may be related to the transport of O_3 from the stratosphere to the troposphere[36]. In addition, meteorological environments with a high ultraviolet intensity and low humidity are conducive to O_3 formation. In general, the formation of O_3 pollution is affected by many factors, including prerequisite pollutant concentrations and meteorological conditions.

Annual variation in O_3 in China. Figure 3 shows the change in ozone concentration in all cities in China in 2016-2018. The top and bottom whiskers extend from the hinges to the largest values by no more than 1.5* IQR (interquartile range). The upper and lower bounds of the box represent the 75th and 25th quartiles, respectively. The line in the middle of the box represents the median. The cross points indicate the mean values, and the square points outside the whisker indicate outliers. From 2016 to 2018, the O_3 concentration showed an upward trend,

2016	2017	2018
1. Beijing (Beijing Municipality)	1. Linfen (Shanxi Province)	1. Baoding (Hebei Province)
2. Tai'an (Shandong Province)	2. Baoding (Hebei Province)	2. Jinan (Shandong Province)
3. Dezhou (Shandong Province)	3. Jincheng (Shanxi Province)	3. Liaocheng (Shandong Province)
4. Hengshui (Hebei Province)	4. Anyang (Henan Province)	4. Binzhou (Shandong Province)
5. Dongying (Shandong Province)	5. Jiaozuo (Henan Province)	5. Jincheng (Shanxi Province)
6. Wuxi (Jiangsu Province)	6. Tai'an (Shandong Province)	6. Dezhou (Shandong Province)
7. Jinzhou (Liaoning Province)	7. Xingtai (Hebei Province)	7. Shijiazhuang (Hebei Province)
8. Jinan (Shandong Province)	8. Langfang (Hebei Province)	8. Xingtai (Hebei Province)
9. Panjin (Liaoning Province)	9. Tangshan (Hebei Province)	9. Cangzhou (Hebei Province)
10. Heze (Shandong Province)	10. Luoyang (Henan Province)	10. Handan (Hebei Province)

Table 2. The top 10 cities with the highest 90th percentile of the maximum daily 8-hour average urban O_3 concentration in 2016-2018 in China.

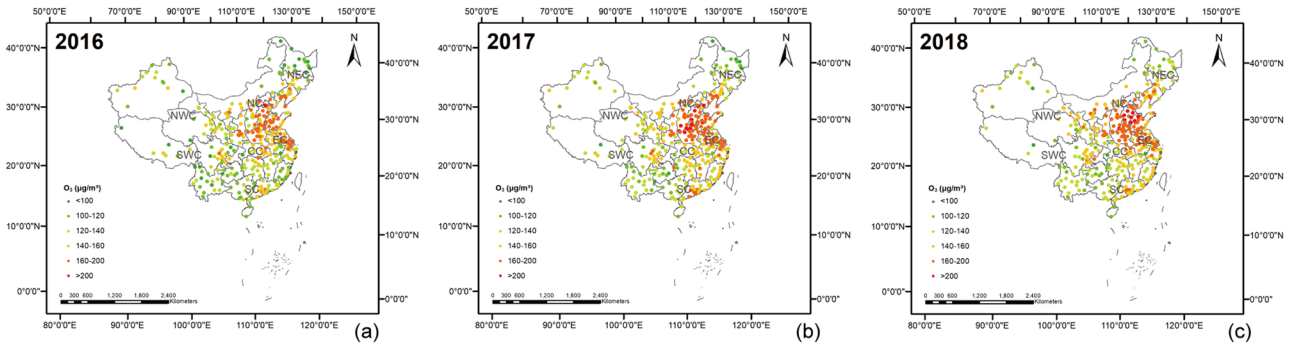

Figure 1. The spatial distribution of the 90th percentile of the maximum daily 8-hour average of the urban O_3 concentration in 338 cities in China in 2016 (**a**), 2017 (**b**), and 2018 (**c**). The maps were generated in ArcGIS10.2, URL: http://www.esrichina-bj.cn/softwareproduct/ArcGIS/.

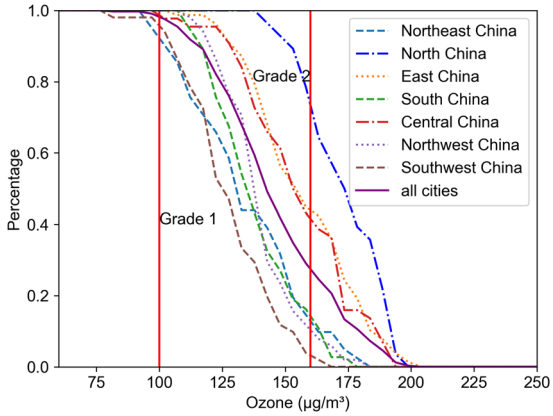

Figure 2. The over-standard rate of O_3 concentration in 338 Chinese cities. The results of the seven geographical regions are also displayed.

and the ozone levels were roughly the same in 2017 and 2018. Figure 1 shows that the scope of heavy O_3 pollution has gradually expanded. This phenomenon is also depicted in Fig. 4. In 2016, more than 95% of cities failed to meet the Grade 1 standard, and nearly 20% failed to meet the Grade 2 standard. In 2017 and 2018, these values increased to 99% and 30%, respectively.

Seasonal variation in O_3 in China. The distributions of O_3 in different seasons were heterogeneous, exhibiting significant seasonal variations. In general, O_3 pollution in the summer is significantly higher than that in winter (Fig. 5). Because the photochemical reaction process is affected by meteorological conditions such as light and temperature, the meteorological conditions in summer are more suitable for photochemical reactions. In contrast, the UV intensity in winter is low, and the photochemical reaction is not enough to form heavy O_3 pollution.

Seasonality is also reflected in spatial variation. In the spring and summer, O_3 pollution is highest in North, East, and Central China. In autumn, O_3 pollution gradually shifts to the south. In winter, national O_3 pollution is relatively mild, and only a small part of South China suffers from O_3 pollution. Overall, the problem of O_3 pollution in the eastern areas is more serious than that in the western areas. The seasonality of O_3 concentration

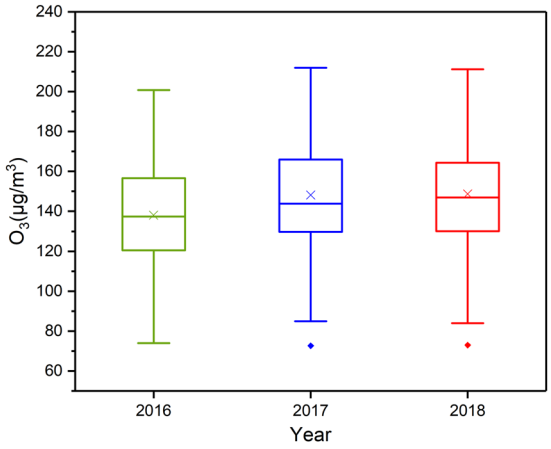

Figure 3. The box plots of the annual O_3 concentrations of 338 cities in China in 2016–2018.

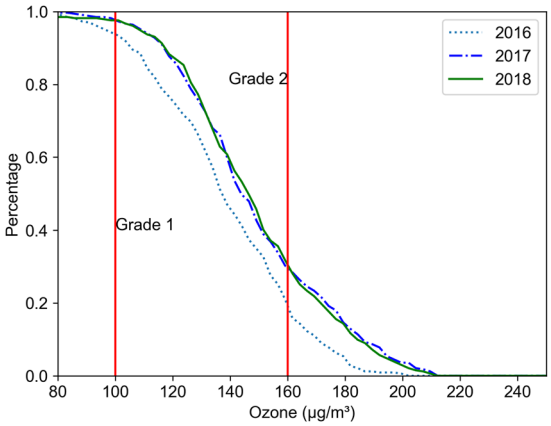

Figure 4. The annual over-standard rate of the O_3 concentrations in 338 Chinese cities in 2016-2018.

changes in the BTH region and the YRD region is relatively high. However, the seasonality of O_3 concentration changes in the PRD region is not as obvious. In the BTH region and the YRD region, the maximum and minimum O_3 concentrations were observed in the summer and winter, respectively. In the PRD region, the maximum O_3 concentration was observed in autumn, and the minimum was observed in winter.

The formation of O_3 pollution varies based on factors such as the overall NO_x and VOC emissions[37–39], topography[40], and atmospheric circulation in the region[31,41]. Evidence suggests that the high O_3 pollution in the BTH region may be related to the emissions of precursor pollutants and the transportation of VOCs in neighboring provinces[42,43]. In the YRD region, the high temperatures in summer and the lower humidity can easily induce O_3 pollution. The O_3 concentration in the PRD region throughout the year is close and at a high level because the temperature throughout the year is similar and the annual average temperature exceeds 20°C in this region.

Monthly variation in O_3 in China. Figure 6 illustrates the highest maximum, upper-quartile, median, lower-quartile, and minimum values of the monthly variations in O_3 concentration from January to December in the seven regions and the total for all cities. The data confirm that the O_3 concentration changes periodically depending on the month. Except for South and Southwest China, the trends in the O_3 concentration variations in other regions are consistent with the national trend, showing an inverted V-shaped curve. The O_3 concentration gradually increases from January to June, reaching the highest value in June, and then gradually decreases from June to December. The trend of O_3 concentration variations in South China and Southwest China is relatively stable. The variation in the O_3 concentration in South China shows an M-shaped curve, and the O_3 concentration is higher in May and October. O_3 pollution in Southwest China is "coming early and going fast". The O_3 concentration peaks around May and then falls sharply starting in June.

The monthly pattern of O_3 can be attributed to changes in meteorological conditions and seasonal variations in precursor emissions. The decrease in the O_3 concentration in South China in summer may be attributed to the climatic characteristic of the southwest monsoon that prevails in summer. The change in the O_3 concentration in Southwest China is strongly affected by ultraviolet radiation. In addition, the penetration of stratospheric ozone into the troposphere is another reason supporting the high O_3 concentration in the region.

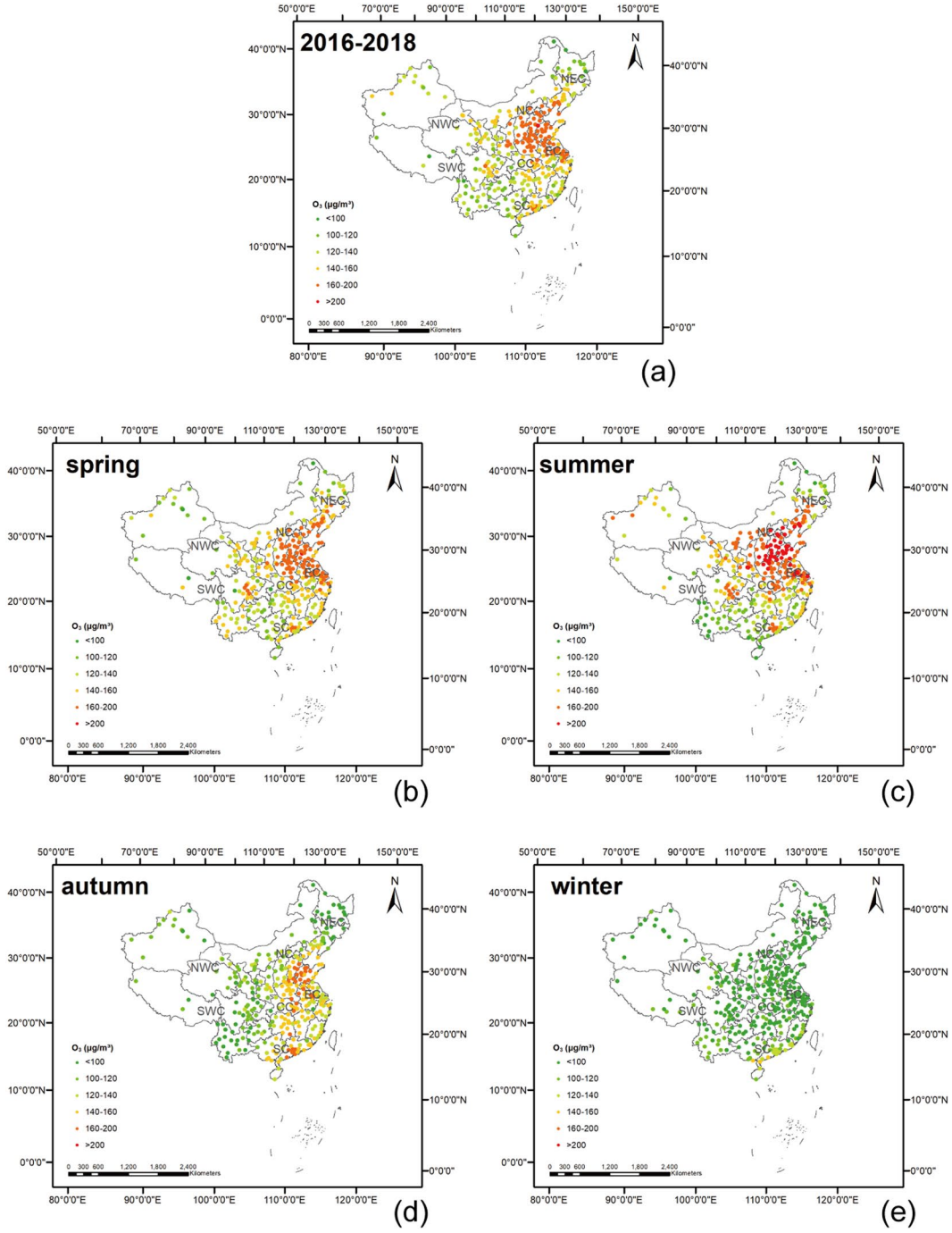

Figure 5. The average O_3 concentrations of the 338 cities of China during 2016, 2017 and 2018 (**a**) and during spring (**b**), summer (**c**), autumn (**d**), and winter (**e**). The maps were generated in ArcGIS10.2, URL: http://www.esrichina-bj.cn/softwareproduct/ArcGIS/.

Weekly variation in O_3 in China. The weekly variation in the O_3 concentration is shown in Fig. 7. The trends in different regions are not the same, but in general, they follow a W-shape. In North, Central, South, and Southwest China and in the BTH and PRD regions, the O_3 concentration showed a valley on Tuesday. In North China, the YRD region, and the BTH region, the O_3 concentration showed another valley on Saturday. Some scholars have studied the weekend effect of O_3 that was first reported in New York in 1974, which suggested that the O_3 concentration was higher during the weekend than on weekdays[44]. The weekend effect has been investigated in many other cities in the United States[45–47], Europe[48–50], and Asia[51–53]. The weekend effect of urban O_3 is related to the decrease in human activities.

As shown in Fig. 8, the weekly variation in O_3 concentration varies greatly in different regions and seasons. In our study, the valley value of O_3 concentration often occurs on Tuesday. The weekend effect of O_3 is more evident in the Northeast China, South China, Central China in summer, and Northwest China, Southwest China in

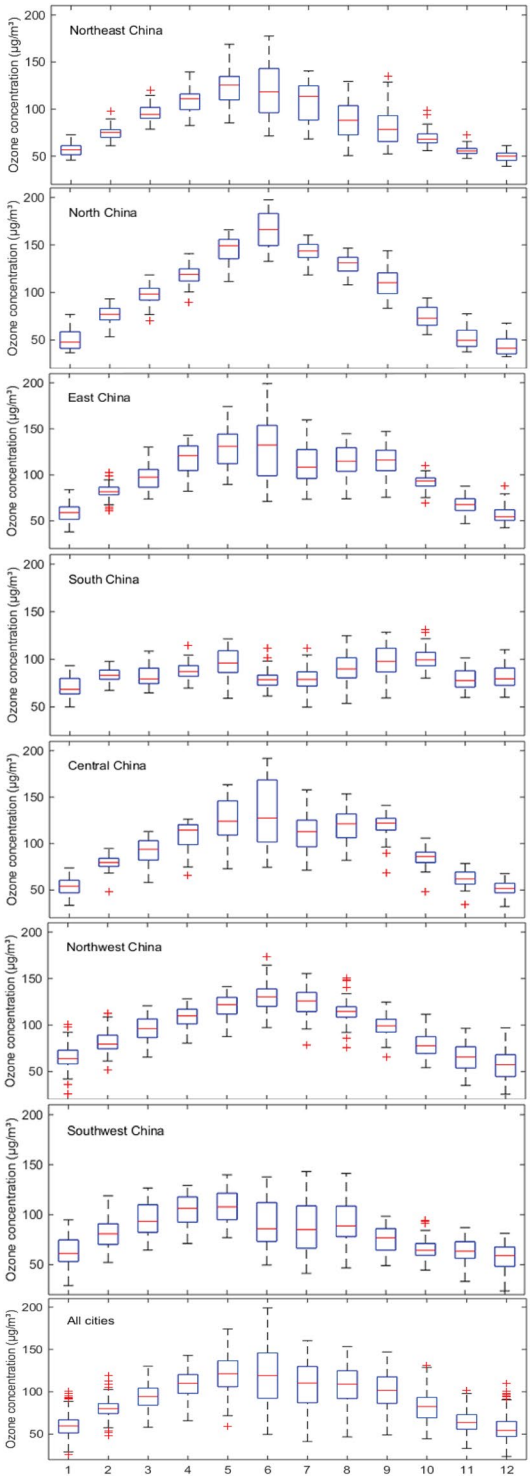

Figure 6. Monthly variation in the maximum daily 8-hour average concentration of O_3 in seven geographical regions and in all cities during 2016-2018.

winter to a certain degree. However, the general weekend effect of O_3 pollution is not significant, from a national scale. The weekly variation in O_3 concentration is affected by complex factors, the most likely of which is characteristics of urban resident activities. At present, no natural process has been found to produce climate change with a cycle of about 7 days, so Dominique *et al.*[54] believe that the existence of such a cyclic process is manifestation of human impact on climate. Due to the obvious weekly cycle of human activities, many meteorological elements in many regions have corresponding weekly cycle characteristics[55]. Meteorological elements of some cities have been observed to have varying degrees of weekly cycle characteristics, such as temperature[56,57], precipitation frequency[58,59], etc., which have a significant cycle with 7-day. The change of these climate factors will further affect

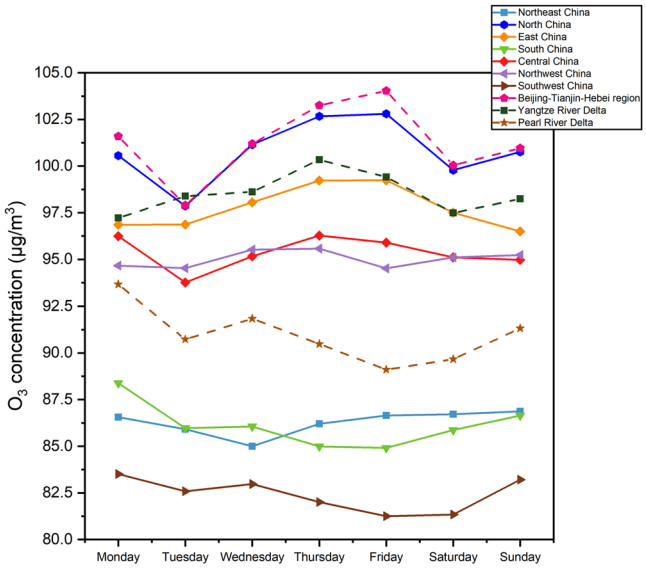

Figure 7. Weekly variation in the maximum daily 8-hour average concentration of O_3 in seven geographical regions and three urban agglomerations in China during 2016-2018.

the generation of O_3 in the photochemical reaction process, and thus affect the weekly variation. In general, the weekly variations in O_3 concentration are not very prominent, which shows that the weekly changes in human activities have limited effects on O_3 concentration.

Daily variation in O_3 in China. Figure 9 shows the daily O_3 concentration from January 1, 2016, to December 31, 2018. As shown in the figure, the daily variation in the O_3 concentration is usually continuous. The change from high concentration to low concentration, or from low concentration to high concentration, is often a gradual process rather than a sudden change. In most parts of the country, the daily variation of O_3 concentration shows an inverse U-shaped trend during each year, i.e., gradually increasing first and then decreasing. Except for South China, including the Pearl River Delta, the daily variation process of O_3 concentration has volatility. When observing horizontally from three years, the three cycles of O_3 variation can be clearly distinguished. We also found that for at least 1/3 of the days in the three years in each region, the O_3 concentration exceeded the AQG, while for more than 1/3 of the days in North China, the O_3 concentration exceeded Grade 1 of the NAAQS. When observing vertically, during the days with O_3 pollution, the BTH, YRD, and PRD regions usually had even higher O_3 concentrations than their neighboring areas. In short, the figure simultaneously shows the seasonal variation pattern as well as the spatial distribution characteristic of O_3 concentration.

Diurnal and nocturnal variation in O_3 in China. The hourly data on O_3 concentration are shown in Fig. 10 and were used to investigate the diurnal and nocturnal variations in O_3 pollutants in seven regions and three urban agglomerations in China. All regions showed a similar overall trend of O_3 concentration, with a single peak. The O_3 concentration was relatively lower at night, but as the sun rose, the O_3 concentration gradually increased. The peak appeared between 14:00 and 16:00 (i.e., in the afternoon). After 16:00, the O_3 concentration gradually decreased. The change in O_3 concentration was affected by the temperature, solar radiation intensity, and various emissions from the surrounding environment. At night, due to the absence of solar radiation and the precursor of the photochemical reaction, the reaction was weakened and the O_3 concentration decreased.

There are still some differences in the diurnal and nocturnal variations in the O_3 concentration in various regions. For example, the variations in Southwest and Northwest China have a hysteresis phenomenon relative to other regions. The phenomenon is attributed to China's vast territory, with more than 60° of east-west longitude, spanning 5,200 km and five time zones. Although Beijing time is uniformly used in China, there are actually time differences between the eastern and western regions.

O_3-NO_x-VOC sensitivity regimes and influencing factors. O_3 is a secondary pollutant, and it is mainly produced by a series of photochemical reactions among precursors. Therefore, the formation of O_3 pollution is affected by many factors in addition to meteorological factors. The most important factors are its precursors NO_x and VOCs. The relationship between O_3 and its precursor concentrations is generally nonlinear[60]. The decrease in precursor concentration does not necessarily result in a corresponding decrease in O_3 concentration, and the sensitivity of O_3 to NO_x and VOCs will be different under different environmental conditions in the same region. The O_3-NO_x-VOC sensitivity regimes can describe the relationship between O_3 and its local precursors (NO_X and VOCs). The sensitivity relationship between O_3 and its precursors determines the controlled types of O_3 pollution in different regions. In brief, when the concentration of NO_x in the atmosphere is high, the generation of O_3 is controlled by VOCs; however, when the VOC concentration in the atmosphere is high, O_3 generation is controlled by NO_x. For example, in VOC-sensitive areas, the O_3 concentration may increase with the reduction of the NO_x concentration[23]. Clarifying whether O_3 generation in a region is VOC-sensitive or NO_x-sensitive is one

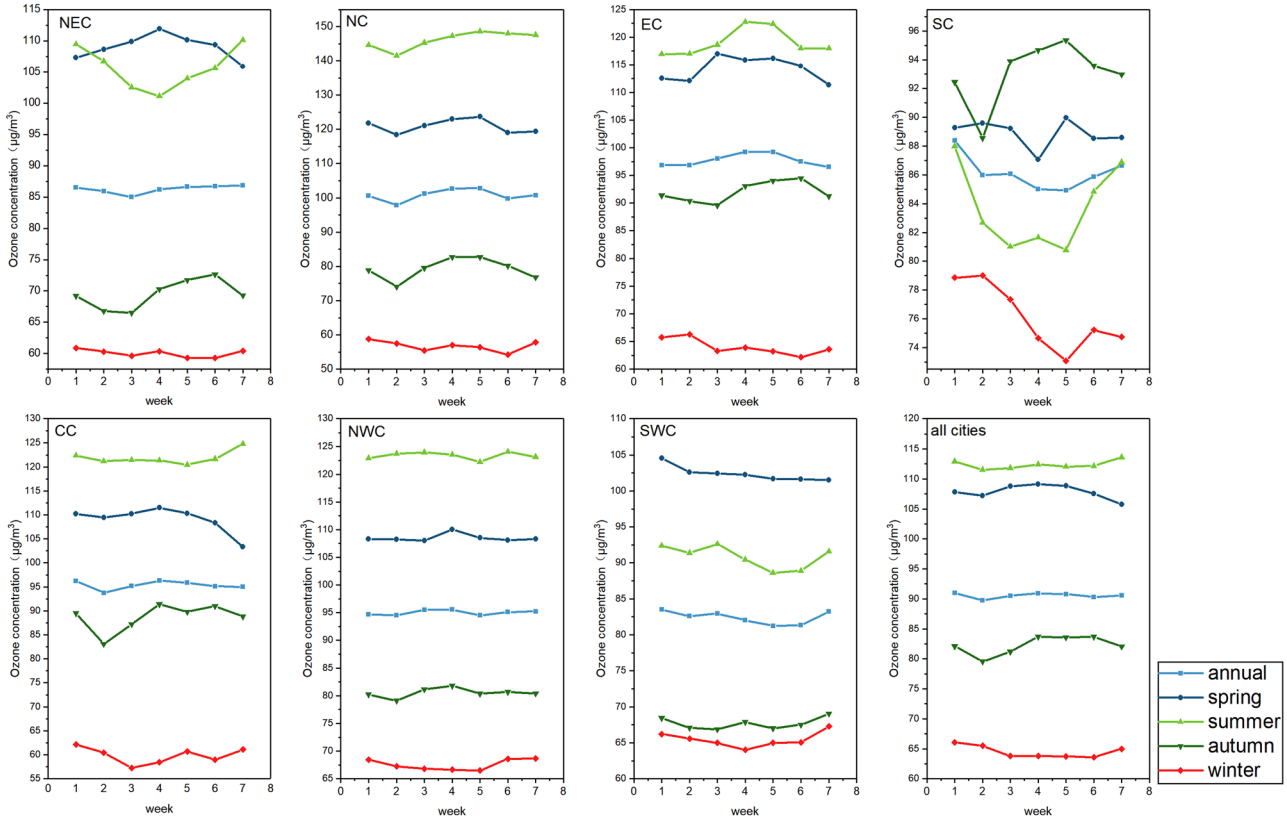

Figure 8. Weekly variation in the maximum daily 8-hour average concentration of O_3 during four seasons in seven geographical regions during 2016-2018.

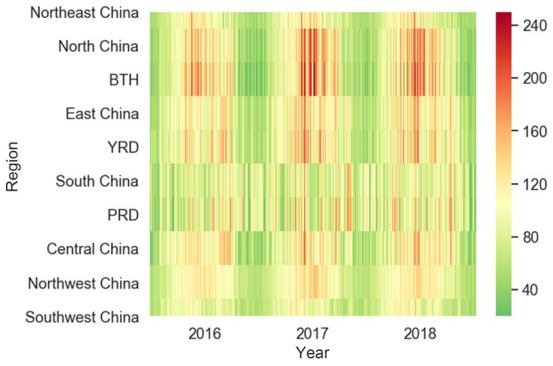

Figure 9. Daily variation in the maximum daily 8-hour average concentration of O_3 in seven geographical regions and three urban agglomerations during 2016-2018. (This figure was created by using matplotlib, a Python 2D plotting library, URL:https://matplotlib.org).

of the important issues related to O_3 generation mechanisms, which will be helpful in determining the control of targeted emissions to reduce O_3 pollution[61] and formulating O_3 pollution control strategies.

In this paper, we summarize the O_3-NO_x-VOC sensitivity regimes in major cities in China that have been studied, and the results are shown in Supplementary Table S1. In the urban districts of most cities, including Beijing, Tianjin, Shanghai and Guangzhou, O_3 generation is VOC-sensitive, mainly because human intervention in urban districts has greatly affected the emissions of precursors. Industry and transportation caused a large amount of NO_x emissions, and the titration effect suppressed the increase in the O_3 concentration in urban areas. In these areas, the priority control of VOC emissions is more helpful in controlling local O_3 pollution. However, in the suburban areas of some cities, such as Lanzhou, Guiyang, Chongqing, and Xuzhou, the generation of O_3 is NO_x-sensitive. The suburbs are less affected by anthropogenic emissions, and the migration of pollutants caused by the wind will affect O_3 pollution in the suburbs. In these areas, to suppress O_3 generation more effectively, priority should be given to the control of NO_x emissions.

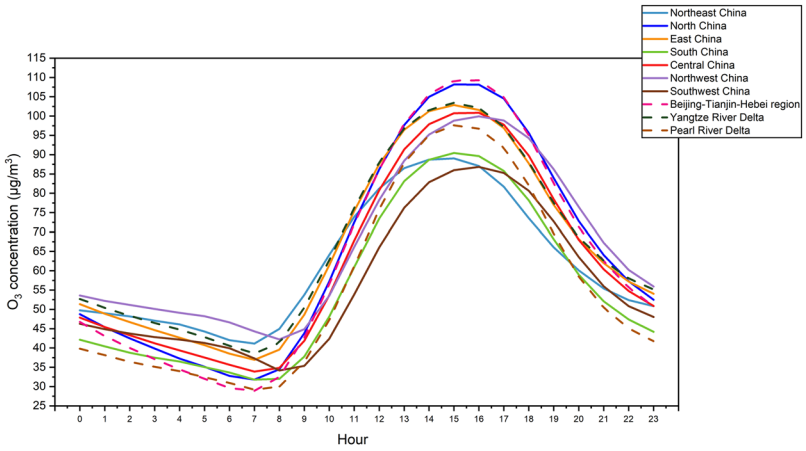

Figure 10. Diurnal and nocturnal variation in the average hourly concentration of O_3 in seven geographical regions and three urban agglomerations during 2016-2018.

In addition, the meteorological influencing factors in major cities in China are provided in Supplementary Table S1. The main meteorological factors that affect O_3 generation include temperature, relative humidity, wind speed, wind direction, solar radiation, atmospheric pressure, cloud cover, sunshine duration, precipitation, ultraviolet radiation, visibility, and geopotential height. The statistics of their frequency are shown in Supplementary Fig. S1. In different regions, meteorological factors have heterogeneous effects on O_3 generation. In general, O_3 has a significant correlation with temperature and relative humidity. High temperature and low relative humidity are more conducive to the formation of O_3, while meteorological factors such as sunshine duration, wind direction and wind speed have a crucial impact on the changes in O_3 concentration.

Combined with the results of previous statistical analyses, we found that the O_3 pollution affecting other cities is often caused by the synergistic effects of precursors and meteorological factors. For example, MDA8 in Beijing and its surrounding areas mainly occur at conditions of high temperature, low cloud cover, low relative humidity, weak southeast wind, low planetary boundary layer height, and the presence of a large amount of NO_x and VOCs[62]. In Taiyuan, when the wind direction is southerly or southwesterly, the concentration of O_3 is higher, which indicates that the increase in O_3 concentration in Taiyuan is not only related to the local generation but also related to the external transport from the south[63,64]. The O_3 volume fraction and its generation rate in Langfang showed a significant positive correlation with air temperature and a significant negative correlation with total cloud cover. It is also susceptible to transmission in the southern region of Hebei and Tianjin.

From a long-term perspective, according to the characteristics of different O_3 pollution in different regions, priority should be given to strengthen the coordinated control of the sensitive precursor emissions in the region. Forecasting in advance when meteorological conditions are adverse and taking timely NO_x and VOC control measures are important ways to solve regional O_3 pollution problems.

Conclusions

This study analyzed the spatiotemporal distributions of O_3 concentrations in 338 prefecture-level cities in China from January 2016 to February 2019. The purpose was to understand the current status of O_3 pollution in China with a higher spatial resolution and a longer time series. Our study has the following findings:

O_3 had obvious spatial heterogeneity. Only a few cities met the AQG standard of the WHO. O_3 pollution in North, East, and Central China was more serious, especially in the BTH region. The O_3 concentrations in the BTH, YRD, and PRD regions were usually higher than those in their neighboring cities. In the spring and summer, O_3 pollution in the north was more serious; in autumn, O_3 pollution shifted toward the south. In winter, the O_3 pollution problem was relatively mild across China.

O_3 showed a significant temporal variation pattern. The O_3 concentration increased each year from 2016 to 2018. For the monthly variation in O_3, except for South and Southwest China, other regions showed an inverted-V curve. Although the weekly variation in O_3 concentration was not exactly the same in different areas, some cities showed a W-shape. The O_3 concentration was lower on Tuesday and Saturday, and no obvious weekend effect was found. The study also characterized the diurnal and nocturnal variation pattern of O_3 concentration. The O_3 concentration was significantly higher during the day because of factors such as solar radiation, temperature, and precursor emissions. Due to the different time zones in different cities, the western region had a remarkable lag effect compared with the eastern region.

At present, China has made some achievements in the control of PM, NOx and other pollutants; however, the problem of O_3 pollution has become increasingly prominent. Against the background of China's severe composite air pollution, the need for the coordinated control of multiple pollutants is becoming increasingly apparent. According to our understanding, there is coexistence of VOC control and NOx control in China's O_3 pollution, and the reduction of particulate matter pollution has exacerbated the problem of O_3 pollution in China. The government should strengthen the monitoring of VOCs and combine the characteristics of O_3 pollution in different regions to formulate more targeted O_3 pollution control strategies to achieve a win-win situation of haze governance and O_3 control.

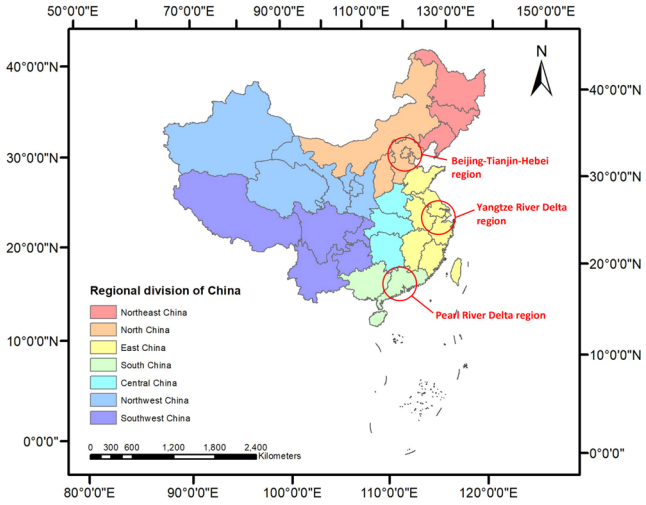

Figure 11. The regional division of China into seven geographical regions and three urban agglomerations. The map was generated in ArcGIS10.2, URL: http://www.esrichina-bj.cn/softwareproduct/ArcGIS/.

Data and methods

The regional division of China. A total of 338 cities, including prefecture-level cities and municipalities, are used as basic study units to investigate the spatial and temporal distribution of O_3 in China. To analyze the results more clearly, China was divided into seven geographical regions: Northeast China (NEC), North China (NC), East China (EC), Central China (CC), South China (SC), Northwest China (NWC), and Southwest China (SWC), and three urban agglomerations: Beijing-Tianjin-Hebei region (BTH), the Yangtze River Delta region (YRD), and the Pearl River Delta region (PRD) (Fig. 11).

Ground-level O_3 monitoring data. The China National Environmental Monitoring Center (CNEMC) continuously operates and maintains the national air quality monitoring network of China. The network has comprised 496 stations in 74 cities since 2012, and the network was extended to 1436 monitoring stations in 338 cities after 2016. The real-time concentration of O_3 was measured by the ultraviolet absorption spectrometry method and differential optical absorption spectroscopy at each monitoring site. The instrumental operation, maintenance, data assurance and quality control were properly conducted based on the most recent revisions of China Environmental Protection Standards[2]. The real-time hourly O_3 concentration data are continuously recorded by the CNEMC in China and are provided to the public. The data for this study were obtained during the period from 1-Jan-2016 to 28-Feb-2019.

Maximum daily 8-hour average O_3 and the annual average O_3 concentration. In view of the impact of long-term O_3 exposure on animals and plants, limits of the maximum daily 8-hour average O_3 concentration are specified in the NAAQS. Therefore, the average hourly O_3 concentration is calculated every 8 hours, which should include at least 6 hourly values within a given 8-hour period; otherwise, the average value is considered to be invalid. Invalid values are not accepted in subsequent analysis. Finally, the maximum daily 8-hour average O_3 concentration in a day is used to represent the O_3 level of that day. Additionally, the 'technical regulation for ambient air quality assessment of China' (on trial) (HJ 633-2013) published by the Ministry of Ecology and Environment of China (MEE) determined that the O_3 annual assessment standard for a city is equal to the 90th percentile of MDA8.

Statistical method. The spatial distribution of O_3 is analyzed by calculating the average MDA8 data of all cities in each region. The annual, seasonal, monthly, weekly and daily variations in O_3 are represented by the average of the MDA8 of each city. Diurnal and nocturnal O_3 variation is calculated using the hourly O_3 concentration of each city.

Received: 29 October 2019; Accepted: 20 March 2020;
Published online: 29 April 2020

References

1. China, M. Ambient air quality standards. GB 3095-2012. China Environmental Science Press, Beijing (2012).
2. Zhang, Y. & Cao, F. Fine particulate matter (PM 2.5) in China at a city level. *SCI REP-UK* **5**, 14884 (2015).
3. An, J., Shi, Y., Wang, J. & Zhu, B. Temporal Variations of O3 and NOxin the Urban Background Atmosphere of Nanjing, East China. *Arch Environ Con Tox* **71**, 224–234 (2016).
4. Jin, Y., Andersson, H. & Zhang, S. Air pollution control policies in China: a retrospective and prospects. *Int J Env Res Pub He* **13**, 1219 (2016).
5. Zhang, H. *et al.* Air pollution and control action in Beijing. *J Clean Prod* **112**, 1519–1527 (2016).

6. Feng, L. & Liao, W. Legislation, plans, and policies for prevention and control of air pollution in China: achievements, challenges, and improvements. *J Clean Prod* **112**, 1549–1558 (2016).
7. Krzyzanowski, M. & Cohen, A. Update of WHO air quality guidelines. *Air Quality, Atmosphere & Health* **1**, 7–13 (2008).
8. Wang, Z. *et al*. Temporospatial variations and Spearman correlation analysis of ozone concentrations to nitrogen dioxide, sulfur dioxide, particulate matters and carbon monoxide in ambient air, China. *Atmos Pollut Res* **10**, 1203–1210 (2019).
9. Cheng, L. *et al*. Regionalization based on spatial and seasonal variation in ground-level ozone concentrations across China. *J Environ Sci-China* **67**, 179–190 (2018).
10. Khaniabadi, Y. O. *et al*. Cardiopulmonary mortality and COPD attributed to ambient ozone. *Environ Res* **152**, 336–341 (2017).
11. Huang, J. *et al*. The burden of ozone pollution on years of life lost from chronic obstructive pulmonary disease in a city of Yangtze River Delta, China. *Environ Pollut* **242**, 1266–1273 (2018).
12. Zhao, T., Markevych, I., Romanos, M., Nowak, D. & Heinrich, J. Ambient ozone exposure and mental health: A systematic review of epidemiological studies. *Environ Res* **165**, 459–472 (2018).
13. Liu, H. *et al*. Ground-level ozone pollution and its health impacts in China. *Atmos Environ* **173**, 223–230 (2018).
14. Tai, A. P. K., Martin, M. V. & Heald, C. L. Threat to future global food security from climate change and ozone air pollution. *Nat Clim change* **4**, 817–821 (2014).
15. Emberson, L. D. *et al*. A comparison of North American and Asian exposure–response data for ozone effects on crop yields. *Atmos Environ* **43**, 1945–1953 (2009).
16. Fuhrer, J. & Booker, F. Ecological issues related to ozone: agricultural issues. *Environ Int* **29**, 141–154 (2003).
17. Broberg, M. C., Uddling, J., Mills, G. & Pleijel, H. Fertilizer efficiency in wheat is reduced by ozone pollution. *Sci Total Environ* **607**, 876–880 (2017).
18. Li, C., Meng, J., Guo, L. & Jiang, G. Effects of ozone pollution on yield and quality of winter wheat under flixweed competition. *Environ Exp Bot* **129**, 77–84 (2016).
19. Pu, X. *et al*. Enhanced surface ozone during the heat wave of 2013 in Yangtze River Delta region, China. *Sci Total Environ* **603-604**, 807–816 (2017).
20. Kerckhoffs, J. *et al*. A national fine spatial scale land-use regression model for ozone. *Environ Res* **140**, 440–448 (2015).
21. Doherty, R. M. Ozone pollution from near and far. *Nat Geosci* **8**, 664–665 (2015).
22. Xue, L. K. *et al*. Ground-level ozone in four Chinese cities: Precursors, regional transport and heterogeneous processes. *Atmos Chem Phys* **14**, 13175–13188 (2014).
23. Wang, T. *et al*. Ozone pollution in China: A review of concentrations, meteorological influences, chemical precursors, and effects. *Sci Total Environ* **575**, 1582–1596 (2017).
24. Xue, L. *et al*. Oxidative capacity and radical chemistry in the polluted atmosphere of Hong Kong and Pearl River Delta region: analysis of a severe photochemical smog episode. *Atmos Chem Phys* (2016).
25. Deng, Y., Li, J., Li, Y., Wu, R. & Xie, S. Characteristics of volatile organic compounds, NO_2, and effects on ozone formation at a site with high ozone level in Chengdu. *J Environ Sci-China* **75**, 334–345 (2019).
26. Wang, W. *et al*. Assessing Spatial and Temporal Patterns of Observed Ground-level Ozone in China. *Sci Rep-UK* **7**, 3651 (2017).
27. Kanda, I. & Wakamatsu, S. Small-scale variations in ozone concentration in low mountains. *Atmos Environ* **184**, 98–109 (2018).
28. Ling, Z. H., Guo, H., Cheng, H. R. & Yu, Y. F. Sources of ambient volatile organic compounds and their contributions to photochemical ozone formation at a site in the Pearl River Delta, southern China. *Environ Pollut* **159**, 2310–2319 (2011).
29. Duan, J., Tan, J., Yang, L., Wu, S. & Hao, J. Concentration, sources and ozone formation potential of volatile organic compounds (VOCs) during ozone episode in Beijing. *Atmos Res* **88**, 25–35 (2008).
30. Wu, W., Zhao, B., Wang, S. & Hao, J. Ozone and secondary organic aerosol formation potential from anthropogenic volatile organic compounds emissions in China. *J Environ Sci-China* **53**, 224–237 (2017).
31. Ning, G. *et al*. Characteristics of air pollution in different zones of Sichuan Basin, China. *Sci Total Environ* **612**, 975–984 (2018).
32. Li, R. *et al*. Spatial and temporal variation of particulate matter and gaseous pollutants in China during 2014–2016. *Atmos Environ* **161**, 235–246 (2017).
33. Ou, S. *et al*. Pollution Characteristics and Sensitivity of Surface Ozone in the Typical Heavy Industry City of North China Plain in Summer. *Envirionmental Science*, 1-13 (2020).
34. Zhang, C. *et al*. Satellite UV-Vis spectroscopy: implications for air quality trends and their driving forces in China during 2005–2017. *Light: Science & Applications* **8**, 100 (2019).
35. de Foy, B., Lu, Z. & Streets, D. G. Satellite NO2 retrievals suggest China has exceeded its NOx reduction goals from the twelfth Five-Year Plan. *SCI REP-UK* **6**, 35912 (2016).
36. Chen, C. *et al*. Vertical distribution of ozone and stratosphere-troposphere exchanges on the northeastern side of Tibetan Plateau. *Plateau Meteorology* **31**, 295–303 (2012).
37. Shiu, C. *et al*. Photochemical production of ozone and control strategy for Southern Taiwan. *Atmos Environ* **41**, 9324–9340 (2007).
38. Guo, H., Cheng, H. R., Ling, Z. H., Louie, P. K. K. & Ayoko, G. A. Which emission sources are responsible for the volatile organic compounds in the atmosphere of Pearl River Delta? Vol. 188. (2011).
39. Cheng, H. *et al*. On the relationship between ozone and its precursors in the Pearl River Delta: Application of an observation-based model (OBM). *Environ Sci Pollut R* **17**, 547–560 (2010).
40. Klingberg, J. *et al*. Variation in ozone exposure in the landscape of southern Sweden with consideration of topography and coastal climate. *Atmos Environ* **47**, 252–260 (2012).
41. Lin, M., Horowitz, L. W., Oltmans, S. J., Fiore, A. M. & Fan, S. Tropospheric ozone trends at Mauna Loa Observatory tied to decadal climate variability. *Nat Geosci* **7**, 136–143 (2014).
42. Zhang, Q. *et al*. Variations of ground-level O 3 and its precursors in Beijing in summertime between 2005 and 2011. *Atmos Chem Phys* **14**, 6089–6101 (2014).
43. Xu, J. *et al*. Measurements of ozone and its precursors in Beijing during summertime: impact of urban plumes on ozone pollution in downwind rural areas. *Atmos Chem Phys* **11**, 12241–12252 (2011).
44. Cleveland, W. S., Graedel, T. E., Kleiner, B. & Warner, J. L. Sunday and workday variations in photochemical air pollutants in New Jersey and New York. *Science* **186**, 1037–1038 (1974).
45. Altshuler, S. L., Arcado, T. D. & Lawson, D. R. Weekday vs. weekend ambient ozone concentrations: Discussion and hypotheses with focus on Northern California. *Journal of the Air and Waste Management Association* **45**, 967–972 (1995).
46. Koo, B. *et al*. Impact of meteorology and anthropogenic emissions on the local and regional ozone weekend effect in Midwestern US. *Atmos Environ* **57**, 13–21 (2012).
47. Seguel, R. J., Morales, S. R. G. E. & Leiva G., M. A. Ozone weekend effect in Santiago, Chile. *Environ Pollut* **162**, 72–79 (2012).
48. Pont, V. & Fontan, J. Comparison between weekend and weekday ozone concentration in large cities in France. *Atmos Environ* **35**, 1527–1535 (2001).
49. Schipa, I., Tanzarella, A. & Mangia, C. Differences between weekend and weekday ozone levels over rural and urban sites in Southern Italy. *Environ Monit Assess* **156**, 509–523 (2009).
50. Castell-Balaguer, N., Téllez, L. & Mantilla, E. Daily, seasonal and monthly variations in ozone levels recorded at the Turia river basin in Valencia (Eastern Spain). *Environ Sci Pollut R* **19**, 3461–3480 (2012).
51. Sadanaga, Y., Shibata, S., Hamana, M., Takenaka, N. & Bandow, H. Weekday/weekend difference of ozone and its precursors in urban areas of Japan, focusing on nitrogen oxides and hydrocarbons. *Atmos Environ* **42**, 4708–4723 (2008).

52. Tan, P. H., Chou, C. & Chou, C. C. K. Impact of urbanization on the air pollution "holiday effect" in Taiwan. *Atmos Environ* **70**, 361–375 (2013).
53. Xie, M. *et al*. Temporal characterization and regional contribution to O_3 and NO x at an urban and a suburban site in Nanjing, China. *Sci Total Environ* **551-552**, 533–545 (2016).
54. Bäumer, D. & Vogel, B. An unexpected pattern of distinct weekly periodicities in climatological variables in Germany. *Geophysical Research Letters - Geophys Res Lett* **35** (2008).
55. Hou, L. & Yao, Z. Air Pollution Index and Precipitation Weekly Circulation Characteristics and Its Possible Influencing Mechanism Analysis over Beijing and Its Adjacent Regions. *Chinese Journal Of Atmospheric Sciences* **36** (2012).
56. Gong, D.Y., Guo, D. & Ho, C.H. Weekend effect in diurnal temperature range in China: Opposite signals between winter and summer. *Journal of Geophysical Research: Atmospheres* **111** (2006).
57. Duan, C., Miao, Q., Ma, L. & Wang, Y. Weekend Effect of Temperature Variation in the Yangtze River Delta Region. *Resources and Environment in the Yangtze Basin* **21** (2012).
58. Gong, D.Y. *et al*. Weekly cycle of aerosol-meteorology interaction over China. *Journal of Geophysical Research: Atmospheres* **112** (2007).
59. Bell, T.L. *et al*. Midweek increase in US summer rain and storm heights suggests air pollution invigorates rainstorms. *Journal of Geophysical Research: Atmospheres* **113** (2008).
60. Yoo, E. & Park, O. A study on the formation of photochemical air pollution and the allocation of a monitoring network in Busan. *Korean J Chem Eng* **27**, 494–503 (2010).
61. Wang, M. Y., Yim, S. H. L., Wong, D. C. & Ho, K. F. Source contributions of surface ozone in China using an adjoint sensitivity analysis. *Sci Total Environ* **662**, 385–392 (2019).
62. Tang, G. *et al*. Spatial-temporal variations in surface ozone in Northern China as observed during 2009–2010 and possible implications for future air quality control strategies. *Atmos Chem Phys* **12**, 2757–2776 (2012).
63. Feng, X. Variation characteristics of ozone concentration in Taiyuan from 2013 to 2017. *Environ Chem* **38**, 1899–1905 (2019).
64. Zhang, S., Zhang, X., Chai, F. & Xue, Z. Pollution Characteristics of NOx, $O_3$and OX in the Ambient Air of Taiyuan City and Relativity Study. *Environmental Protection Science* **41**, 54–58 (2015).

Acknowledgements

This work is supported by the National Natural Science Foundation of China (71671024, 71601028, 71421001), Fundamental Research Funds for the Central Universities (DUT20JC38, DUT20RW301), Humanity and Social Science Foundation of the Ministry of Education of China (15YJCZH198), Social Planning Foundation of Liaoning (L17AGL012), and Scientific and Technological Innovation Foundation of Dalian (2018J11CY009). The authors would like to thank the reviewers for their constructive comments.

Author contributions

G.F.Y. and Y.H.L. designed and performed the research. G.F.Y. and Y.H.L. wrote the manuscript and checked the Analysis. X.N.L. reviewed the analysis and revised the manuscript.

Competing interests

The authors declare no competing interests.

Additional information

Supplementary information is available for this paper at https://doi.org/10.1038/s41598-020-64111-3.

Correspondence and requests for materials should be addressed to G.Y.

Reprints and permissions information is available at www.nature.com/reprints.

Publisher's note Springer Nature remains neutral with regard to jurisdictional claims in published maps and institutional affiliations.

Open Access This article is licensed under a Creative Commons Attribution 4.0 International License, which permits use, sharing, adaptation, distribution and reproduction in any medium or format, as long as you give appropriate credit to the original author(s) and the source, provide a link to the Creative Commons license, and indicate if changes were made. The images or other third party material in this article are included in the article's Creative Commons license, unless indicated otherwise in a credit line to the material. If material is not included in the article's Creative Commons license and your intended use is not permitted by statutory regulation or exceeds the permitted use, you will need to obtain permission directly from the copyright holder. To view a copy of this license, visit http://creativecommons.org/licenses/by/4.0/.

© The Author(s) 2020